Anisotropic Strength Model for Stability Analysis on Metasedimentary Sandstone-Shale Rock Slope: A Case Study

Mohd Mustaqim Mohd-Nordin[1,2], Mohd Ashraf Mohamad Ismail[1(✉)], and Mazlina Razali[1,3]

[1] School of Civil Engineering, Universiti Sains Malaysia, Engineering Campus, Nibong Tebal, Penang, Malaysia
ceashraf@usm.my
[2] Civil Engineering Studies, College of Engineering, Universiti Teknologi MARA (Pahang), Bandar Tun Abdul Razak, Jengka, Malaysia
[3] Civil Engineering Studies, College of Engineering, Universiti Teknologi MARA (Penang), Permatang Pauh, Penang, Malaysia

Abstract. The anisotropic geological setting has a predominant multi-orientation of weakness planes that are integrated with the matrix structure of major joint sets. The sedimentary bedding orientation and shear surface resistance significantly governed the plane's deformation characteristics and, thus, the mode of failure. In this study, the metasedimentary sandstone-shale interbedded rock slope at Gubir, Kedah, the north of Malaysia Peninsula, was examined. The rock slope formation is calculated for the factor of safety (FoS) using the 2D limit equilibrium method (LEM) by employing an anisotropic geomaterial with a directional strength model. The 2D rock slope geometrical profile was extracted from the Structure from Motion (SfM) point cloud photogrammetry images. The geological description and local geostructural characteristics for the study area were recognised based on the bedding characterization and rock material identification. The interpretation with the probabilistic factor of failure to increase confidence in the input parameter values that were assigned and consider the uncertainty for these values. Accordingly, the Mohr-Coulomb strength parameters of bedding material were identified as the main contribution to controlling the failure potential. The sensitivity analysis has proven the critical level of these variable parameters for the failure of the slope, or else for the safer slope. This stability analysis result was validated by the shear strength reduction result in the Finite Element Method (FEM) simulation. The range area of the shear band representing the maximum shear strain shows similar failure behaviour with the minimum FoS determined by GLE/Morgenstern-Price, thus validating the results obtained.

Keywords: Anisotropic Strength Model · Stability Analysis · Interbedded Rock Slope

R. E. Hammah et al. (Eds.): RIC 2023, AHE 19, pp. 770–782, 2023.
https://doi.org/10.2991/978-94-6463-258-3_71

1 Introduction

An anisotropic formation introduces a plane of weakness compared to the rock matrix and has prominently lower strength and higher compressibility. According to [1], rock mass anisotropy can be classified into structural anisotropy and inherent anisotropy. Structure anisotropy is mostly related to discontinuities in a rock mass, and examples are bedding and lamination formation. Inherent anisotropy is related to the texture or fabric of intact rock, which is governed by the orientation of mineral grains such as fissility and foliation.

Fracture distribution and characteristics of the bedding planes influence the bedding shear strength of the interbedded rock slope. Saturation plays a significant role in bedding shear strength [2], thus progressively weakening the Mohr-Coulomb strength parameters that describe the shear strength of weathering grades responsible for failure of weak layers.

The shear strength of intact rock is defined in terms of major and minor principal stress acting upon the rock mass element. The failure criterion model was extended further by [3], where the additional factor of the discontinuity element is considered due to erroneous result by assuming Hoek-Brown failure criterion for anisotropic conditions. A practical method to estimate rock mass strength and deformability using the Hoek-Brown failure criterion in heavily jointed rock masses was improvised by [4] as stated in Eq. 1.

$$\sigma_1' = \sigma_3' + \sigma_c \left(m_b \frac{\sigma_3'}{\sigma_c} + s \right)^a \tag{1}$$

The rock mass characteristic applicable to estimate the strength and deformability of jointed rock masses derived from Geological Strength Index (GSI) by [5], compressive strength, σ_c for rock material, and m_b constant for rock material. For intact rock, the rock mass characteristics $s = 0$ and $a = 0.5$, where these two attribute parameters define the Hoek-Brown failure envelope according to UCS of intact rock material and intact material parameter, m_i. Two main assessment factors in GSI chart are the geological structure and rock joint surface conditions, mainly governed the classification rating index, thus representing the changes of geological conditions. For anisotropy or unique rock mass characteristic, the following Eq. (2) to Eq. (4) are applicable for a better empirical values of rock mass constants parameters, i.e. m_b, s and a [6].

$$m_b = m_i \, exp\left(\frac{GSI - 100}{28 - 14D} \right) \tag{2}$$

$$s = \exp\left(\frac{GSI - 100}{9 - 3D} \right) \tag{3}$$

$$a = \frac{1}{2} + \frac{1}{6}\left(e^{-\frac{GSI}{15}} - e^{-\frac{20}{3}} \right) \tag{4}$$

The shear strength of an anisotropic rock mass was well described in anisotropic strength models by improving the different material types and shear direction [7]. There are different shear mechanisms for anisotropic material, particularly either sheared at

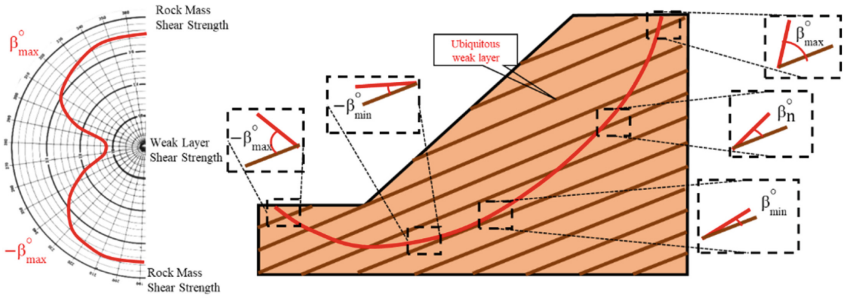

Fig. 1. Graphical illustration for directional shear strength model application correspond to AoA with potential slip failure orientation

positive or negative side for Angle of Anisotropy (AoA). The shear strength depends not only on the magnitude of the anisotropy direction, but also on the shear direction of rock lamellae. The strength of anisotropy planes and orientation of anisotropy are two main components in the directional strength model [8]. The directional shear strength model allows the application of different shear strengths to different slip surface orientation [9], (see Fig. 1). This ubiquitous joint model require three main elements: the shear strength of intact rock, the shear strength of anisotropy plane, and the shear strength of the transition between intact rock and the anisotropy plane.

Generalized Anisotropic (GA) model is one of the directional shear strength models for anisotropic rock slope offered in Limit Equilibrium (LE) of Slide by Rocscience software company. The shear strength orientation from the bedding plane can be customized with the functions of bedding dip uncertainty and material transition parameter. The different employment of directional strength model method significantly results in a variant output on factor of safety. In this study, the GA model is employed to represent the composite behaviour of anisotropy rock formation between the host rock and the bedding interval. Further analyses were also presented for probabilistic factors and sensitivity of variable parameters constituent in the Mohr-Coulomb strength model representing the bedding formation due to greater potential in weakening progress by weathering exposure.

2 Study Area

A section of interbedded outcrop that consists of two different rock types was selected for this case study of anisotropic stability analysis. The identification of the rock slope location was made based on existing geological data and an outcrop exposed on the rock slope at Gubir, near to Muda Dam, Kedah State, Malaysia.

2.1 Geological Description

The location of Gubir in the district of Sik, Kedah State, is made up of weathered zones where sandstone and paraquartzite derived from sandstone formed interbedded with shale. An overview of geological setting for the study area as illustrated in Fig. 2.

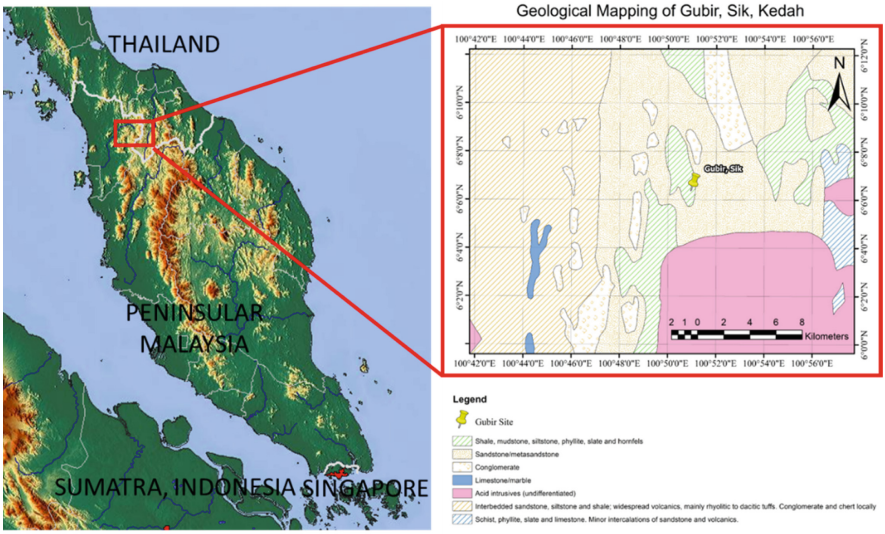

Fig. 2. Location of study area and respective geological formation

The sedimentary origin of rock formations in the Muda Dam vicinity area generally is highly indurated coarse-grained quartzite, while fine-grained rock is variable in composition and more convenient to refer as shale and mudstone [10]. Further findings conclude the geological setting of the area may be divided into two units of sedimentary sequences consisting of alternating quartzites and shale bands that consist of thin quartzite layers. Petrographic analysis indicates the mineralogical texture that confirmed the characteristic of fine-grained size of mainly greyish color of mica and quartz fragment (see Fig. 3).

The configuration between quartzite and sandstone, where a significant difference clearly captured on grained size and structure arrangement due to metamorphism experienced by quartzite. Sutured grains and some quartz recrystallization into triple-junctions typical of compaction during deep burial, rather than a true quartzite derived from the

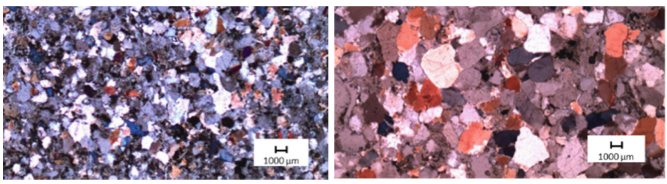

(a) (b)

Fig. 3. Typical petrographic images indicate the difference of grain boundary interaction, (a) Metasedimentary Sandstone (Quartzite), and (b) Sandstone, the composition was estimated as Quartz (~65%), Hematite (~23%), Muscovite (~12%)

intense temperature and pressure changes associated with true metamorphic rock formation. Quartz grains are sutured, but still largely equidimensional and not smeared out with elongated axes.

2.2 Geological Structure Characteristics

Figure 4 illustrates the layer characteristics observed on the slope face, comprising an alternating sequence of interbedded shale with sandstone and paraquartzite formation.

The application of Structure from Motion (SfM) to extract the photogrammetry data into geological planes orientation of interbedded layer was adopted as recommended by [11]. Thus, this complex structural behaviour of the anisotropy formation was well figured up in stereographical plot using Dip software program by Rocscience.

3 Anisotropic Modelling

The slope profile was initially measured by capturing the slope angle and morphology altitude using the surface profile function applicable in DroneDeploy software program. Thus, enable to replicate for 2D model geometry in Slide2 software program by Rocscience. The 2D slope geometry for the LEM analysis with an appropriate boundary conditions and surface analysis (see Fig. 5).

The input values for material properties were adapted from the average range of values summarized from previous studies (see Table 1). The onsite geotechnical description for the rock slope that was mainly considered for GSI assessment was summarized as in Table 2. The strength model for intact rock material is defined based on generalized Hoek-Brown with consideration by Geological Strength Index (GSI), rock material and rock mass characteristic value, m_i. The rock material model for anisotropic characteristic was created by assigning the generalized anisotropic as a directional shear strength

Fig. 4. Typical field sketch of outcrop locality for the rock slope and respective stereographic plots interprets for kinematic analysis planar sliding (dip angle average at 20° ± 10°)

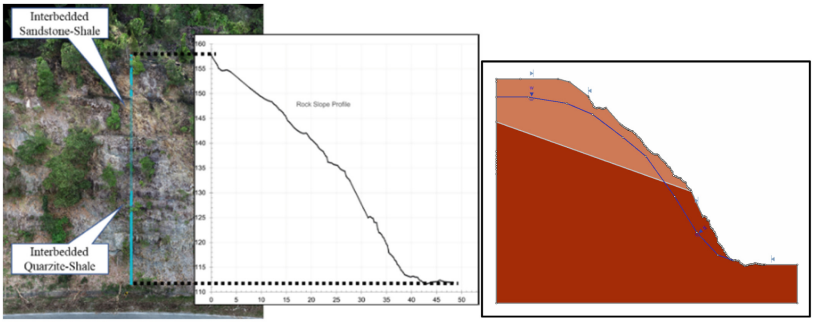

Fig. 5. Surface geometry measurement using DroneDeploy program to capture the actual two-dimensional (2D) profile of rock slope section

model of composite material (see Table 3 and Fig. 6). The combination of different material for a strength model then input with respective range of bedding angle.

4 Numerical Simulation Analyses

There are two types of analyses, both are LEM analysis using Slide2 program and FEM analysis using RS2, both are by Rocscience. Further analysis for probabilistic and sensitivity analyses then detailed for the result interpretation on FoS calculation.

4.1 LEM for FoS and PoF

Analyzing safety factors and probability of failure are the ultimate goals for the interpretation of rock slope stability calculations. The combination between linear and non-linear failure criteria are relevant to optimize both material failure characteristics. The limit equilibrium analysis method using the GLE/Morgenstern-Price and generalized anisotropy function as directional shear strength model result in a FoS of 1.552 on the interbedded metasedimentary sandstone-shale rock slope (see Fig. 7).

The non-circular slip surface for the failure type was predicted along the shale interfaces plane. The deeper position of failure planes on slope may be induced when the FoS increases to 1.60. The safety factor indicates a sound and stable of rock mass although the identification of failure base was within the shale material. Thus, the probabilistic analysis then extended to focus on this rock type on the model.

Probabilistic analysis increases the confidence in the input parameter values that assigned and counter the uncertainty in these values. The main contribution for controlling the failure potential comes from the shale bedding strength parameters as defined by Mohr-Coulomb criterion. This is due to an active material characteristic to response with the weathering exposure due to expansive clay content in shale [22]. The probabilistic sampling method is applied and the relative frequency with respect to the FoS distribution between the range below and above determined FoS is presented (see Fig. 8).

As shown in Fig. 9, both plot of Fig. 9(a) and Fig. 9(b) show the distribution of Mohr-Coulomb strength parameters, i.e., cohesion and friction angle respectively, with

Table 1. Summary for the value range of shale, sandstone, and quartzite material properties

Rock Type	Unit Weight (kN/m^3)	UCS (MPa)	Is(50) (MPa)	*v*	E (GPa)	Mohr-Coulomb		Source
						Phi (°)	C (kPa)	
Shale	20 – 25	<10	0.1 – 0.3	–	20	25 – 35	1 – 20	[12]
	–	–	3.24 – 5.2	–	–	–	–	[13]
	–	8	–	–	1 – 3	–	–	[14]
	23.4	–	–	0.23	–	20 – 25	15	[15]
	–	–	–	–	–	20 – 27	-	[16]
	23.0	8	2.7	0.23	10	28	7.5	Avg.
Sandstone	22 – 23.8	–	–	–	–	–	–	[17]
	–	–	6.5 – 7.3	–	–	–	–	[13]
	18 – 23	10 – 20	0.3 – 1.0	0.2	40	25 – 35	1 – 20	[12]
	22 – 26	80 – 110	1 – 3	0.3	50	35 – 45	10 – 30	[12]
	–	–	–	–	–	27 – 34	–	[16]
	22.96	20 – 172	2 – 11.5	–	–	–	–	[18]
	24.0	91.0	6.0	0.25	45	35	15	Avg.
Quartzite	23 – 25	80 – 110	8 – 10	–	150	30 – 40	20 – 40	[12]
	–	90 – 120	–	–	–	–	–	[19]
	–	46 – 141	–	–	–	–	–	[20]
	27.7	100	–	0.25	42	–	–	[21]
	26.0	98.38	9.0	0.25	95	35	30	Avg.

respect to the value of FoS. The data were divided between lower and higher safety factor of 1.552 (as determined by initial LEM calculation). The correlation coefficient for the point distribution for FoS less than 1.552 indicated by cohesion and friction angle parameters are 0.58 and 0.79 respectively. Hence, the result for FoS value potentially slightly decreased as low as 1.40 and remained stable.

Table 2. Typical geotechnical description parameters defined for GSI input parameters

Rock type	Unit Weight (kN/m^3)	Failure criteria	Anisotropy angle	Geological description
Sandstone	24	Generalized Hoek-Brown	–	Angular blocky and interlocked formed by at least four joint sets
Quartzite	26	Generalized Hoek-Brown	–	
Shale	23	Mohr-Coulomb	10° – 30°	Very weak and highly anisotropic

Table 3. Assigned material with respective strength and properties configuration

Material Name	Color	Unit Weight (kN/m^3)	Strength Type	Remark
Quartzite		26.0	Generalized Hoek-Brown	UCS: 98 000 kPa GSI: 65; m_i: 20; d: 0.7
Shale		23.0	Mohr-Coulomb	Cohesion: 7.5 kPa Phi: 28°
GA in Quartzite		24.5	Generalized Hoek-Brown	Generalized Anisotropic of Quartzite-Shale (see Fig. 6b)
Sandstone		24.0	Generalized Hoek-Brown	UCS: 91 000 kPa GSI: 65; m_i: 17; d: 0.7
GA in Sandstone		23.5	Generalized Hoek-Brown	Generalized Anisotropic of Sandstone-Shale (see Fig. 6a)

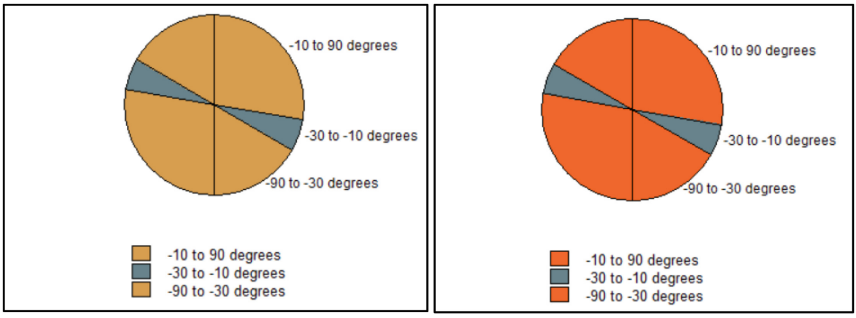

(a) (b)

Fig. 6. The angle range of AoA input defines the generalize anisotropic function, (a) composite material of sandstone and shale, and (b) composite material of quartzite and shale

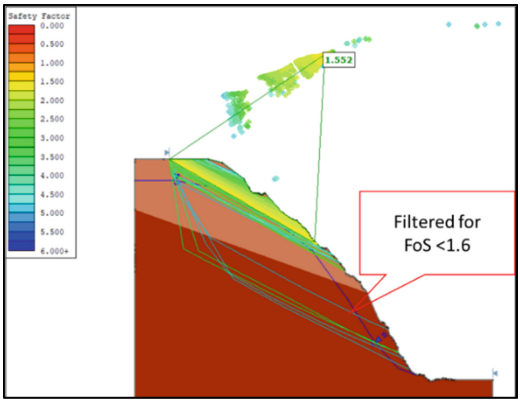

Fig. 7. Factor of safety based on critical non-circular of GLE/Morgenstern-Price generated in Slide2

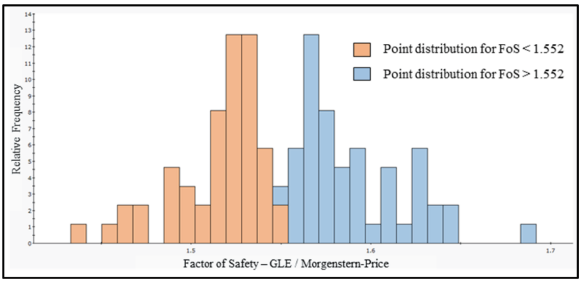

Fig. 8. Distribution of FoS point data with mean = 1.552, standard deviation = 0.04736, minimum = 1.433 and maximum = 1.692

4.2 FEM for Deformation Characterization

A similar slope geometrical model was imported from Slide2 into RS2 and applied similar material properties during the LEM analysis. The input for material properties in RS2 were also assigned similarly during the LEM model generation in Slide2, thus relevant for verification. This comparison between the FoS in LEM analysis with the shear strength reduction factor in FEM analysis introduces a good verification approach for numerical simulation reliability. The superimposed of failure plane on the contour range of maximum shear strain indicate a good agreement for both analyses (see Fig. 10).

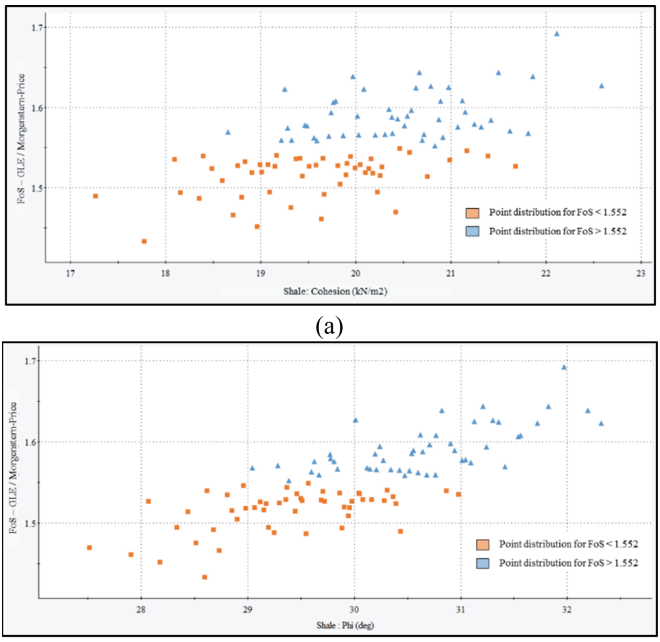

Fig. 9. The main contribution for controlling the failure potential comes from the bedding Mohr-Coulomb strength parameters, (a) cohesion, and (b) friction angle

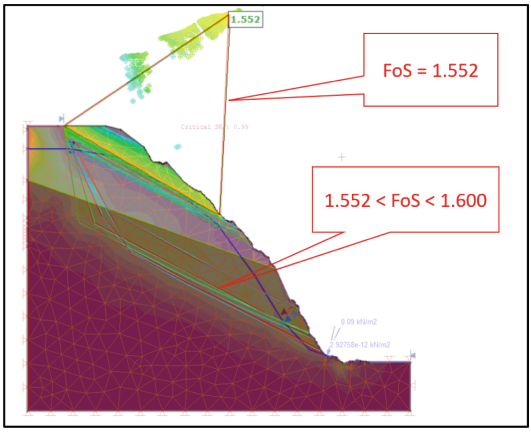

Fig. 10. Similar behaviour between GLE/MP from LEM and FEM superimposed

5 Conclusion

Geological structure input is important to be simulated in numerical simulation stability analysis, especially for anisotropy conditions. The directional shear strength model plays important roles in similarly modeling anisotropic rock slope deformability behaviors.

The high degree of anisotropy is potentially well exhibited with directional shear strength model to account for a range of AoA during numerical model generation. Because of the broad coverage of the GSI classification that takes into account the rock mass strength parameters and discontinuity attributes, the Generalized Hoek-Brown failure criterion can be assigned as the constitutive model for the intact rock material in anisotropy circumstances. Application of realistic geometry to a 2D slope profile results in an appropriate output of stability analysis. The method of utilizing the point cloud from 3D photogrammetry image data idealizes the actual morphology of the slope profile. In fact, the plane extraction yielded accurate and comprehensive information about discontinuity orientation, extending the stability result interpretation to include kinematic stability analysis.

Understand the main bedding material contribution factor in order to predict the potential failure mechanism of an interbedded rock slope. The effect of the degree of deterioration on the bedding material strength on the rock mass stability can be quantitatively estimated based on the statistical figures. The extended analysis of probability of failure and sensitivity analysis for most critical variable parameters introduces a better understanding of uncertainty to the result obtained. The comparison between the FoS in LEM analysis and the shear strength reduction factor in FEM analysis was a good validation instrument in numerical slope stability analysis. The most critical failure plane's position was confidently established, and it was in good agreement with the shear band characteristic representing the maximum shear strain of rock mass deformability. Hence, a systematic concept and empirical approach to analyze the stability analysis for anisotropy of an interbedded rock slope were well established.

Acknowledgement. A great appreciation to Centre of Excellence for Engineering and Technology (CREaTE) JKR Malaysia for the financial support on the laboratory and fieldwork under the Grant No.: 304.PAWAM.6050482.J111. Special thanks also to School of Civil Engineering, Universiti Sains Malaysia for laboratory accessibilities and facilities provided.

References

1. C. Saroglou, S. Qi, S. Guo, and F. Wu, "ARMR, a new classification system for the rating of anisotropic rock masses," Bulletin of Engineering Geology and the Environment, vol. 78, no. 5, pp. 3611–3626, Jul. 2019, doi: https://doi.org/10.1007/s10064-018-1369-4.
2. C. Zhou et al., "Classification of red-bed rock mass structures and slope failure modes in south china," Geosciences (Switzerland), vol. 9, no. 6, Jun. 2019, doi: https://doi.org/10.3390/geosciences9060273.
3. E. Hoek and E. T. Brown, "The Hoek-Brown failure criterion - a 1988 update," in 15th Canadian Rock Mechanics Symposium, 1988, pp. 31–38. [Online]. Available: https://www.researchgate.net/publication/247896456.
4. E. Hoek and E. T. Brown, "Practical estimates of rock mass strength," International Journal of Rock Mechanics and Mining Sciences, vol. 34, no. 8, pp. 1165–1186, Dec. 1997, doi: https://doi.org/10.1016/S1365-1609(97)80069-X.

5. E. Hoek, P. Marinos, and M. Benissi, "Applicability of the geological strength index (GSI) classification for very weak and sheared rock masses. The case of the Athens Schist Formation," Bulletin of Engineering Geology and the Environment, vol. 57, no. 2, pp. 151–160, 1998, doi: https://doi.org/10.1007/S100640050031.
6. E. Hoek, C. Carranza-Torres, and B. Corkum, "Hoek-Brown failure criterion-2002 Edition," in Proceedings of the 5th North American Rock Mechanics Symp., Toronto, Canada, 2002, vol. 1, pp. 267–273. Accessed: Mar. 22, 2023. [Online]. Available: www.rocscience.com.
7. K. G. Mercer, "The History and Development of Anisotropic Linear Model: Part 1," Australian Centre for Geomechanics Newsletter, Vol. 38, July 2012, Nedland, WA, pp. 13–16, 2012.
8. P. Fortsakis, K. Nikas, V. Marinos, and P. Marinos, "Anisotropic behaviour of stratified rock masses in tunnelling," Eng Geol, vol. 141–142, pp. 74–83, Jul. 2012, doi: https://doi.org/10.1016/J.ENGGEO.2012.05.001.
9. C. Saroglou and N. Bar, "The ARMR classification system and the modified hoek-brown failure criterion compared to directional shear strength models for anisotropic rock masses," Periodica Polytechnica Civil Engineering, vol. 64, no. 1, pp. 14–19, Feb. 2020, doi: https://doi.org/10.3311/PPci.14767.
10. C. L. Clarke, S. William Halcrow, U. P. Kirgdrm M JAMES, and R. Student, "Foundation Conditions at Muda Dam," in 2nd ISRM Congress, 1970. [Online]. Available: http://onepetro.org/isrmcongress/proceedings-pdf/CONGRESS70/All-CONGRESS70/ISRM-2CONGRESS-1970-231/2803275/isrm-2congress-1970-231.pdf/1.
11. S. K. Nagendran, M. A. M. Ismail, and W. Y. Tung, "2D and 3D rock slope stability assessment using limit equilibrium method incorporating photogrammetry technique," Bulletin of the Geological Society of Malaysia, vol. 68, pp. 133–139, Dec. 2019, doi: https://doi.org/10.7186/bgsm68201913.
12. B. G. Look, Handbook of Geotechnical Investigation and Design Tables. Taylor & Francis Group, London, UK, 2007.
13. D. Z. Abang Hasbollah et al., "Comparison study on the strength index of tropical shale and sandstone influenced by moisture content," in IOP Conference Series: Materials Science and Engineering, 2019, vol. 527, no. 1. doi: https://doi.org/10.1088/1757-899X/527/1/012041.
14. M. Josh, L. Esteban, C. Delle Piane, J. Sarout, D. N. Dewhurst, and M. B. Clennell, "Laboratory characterisation of shale properties," J Pet Sci Eng, vol. 88–89, pp. 107–124, Jun. 2012, doi: https://doi.org/10.1016/J.PETROL.2012.01.023.
15. W. Zhao, Y. Liu, T. Wang, P. G. Ranjith, and Y. Zhang, "Stability analysis of wellbore for multiple weakness planes in shale formations," Geomechanics and Geophysics for Geo-Energy and Geo-Resources, vol. 7, no. 2, May 2021, doi: https://doi.org/10.1007/s40948-021-00228-7.
16. D. C. Wyllie and N. I. Noiuish, "Rock Strength Properties And Their Measurement," in Rock Slope Engineering, 5th Edition., Duncan C. Wyllie, Ed. CRC Press, 2017, pp. 372–390.
17. I. Komoo and K. A. Kassim, "Influence of moisture content on the strength of weathered sandstone," 2008. [Online]. Available: https://www.researchgate.net/publication/44161123.
18. A. Basu, D. A. Mishra, and K. Roychowdhury, "Rock failure modes under uniaxial compression, Brazilian, and point load tests," Bulletin of Engineering Geology and the Environment, vol. 72, no. 3–4, pp. 457–475, Dec. 2013, doi: https://doi.org/10.1007/s10064-013-0505-4.
19. T. Singh, A. Jain, and K. S. Rao, "Rock failure pattern under uniaxial, triaxial compression and brazilian loading conditions," in Lecture Notes in Civil Engineering, vol. 13, Springer, 2019, pp. 241–249. doi: https://doi.org/10.1007/978-981-13-0368-5_26.
20. V. Gupta and R. Sharma, "Relationship between textural, petrophysical and mechanical properties of quartzites: A case study from northwestern Himalaya," Eng Geol, vol. 135–136, pp. 1–9, May 2012, doi: https://doi.org/10.1016/J.ENGGEO.2012.02.006.

21. T. Singh, A. Jain, and K. S. Rao, "Physico-mechanical Behaviour of Metamorphic Rocks in Rohtang Tunnel, Himachal Pradesh, India," Procedia Eng, vol. 191, pp. 419–425, 2017, doi: https://doi.org/10.1016/J.PROENG.2017.05.199.
22. S. G. Fityus, M. Jeffery, K. J. Aglias, J. A. Johnston, and J. V. Simmons, "Weathering and Degradation of Shales and Mudrocks." OnePetro, May 10, 2015. Accessed: Mar. 24, 2023. [Online]. Available: /isrmcongress/proceedings-abstract/CONGRESS13/All-CONGRESS13/165939.